Analytical Methods

RSC Publishing

PAPER

Mercury emissions in equilibrium: a novel approach for the quantification of mercury emissions from contaminated soils

Manuel Carmona,[a] Williams Llanos,[bc] Pablo Higueras*[c] and David Kocman[d]

Mercury emissions from soil samples with different mercury contents have been estimated using a closed circuit array. The samples were collected from the Almadén mercury mining district. The emissions confirmed that temperature and light radiation favour mercury desorption due to the increase in the mercury vapour pressure. An additional positive factor could be the photocatalytic reduction of soluble Hg^{2+} to volatile Hg^0 at the soil surface. A physicochemical model based on mass transfer and equilibrium was developed and was used to reproduce the mercury emissions at the laboratory scale. The use of this model allowed us to obtain the unknown mass transfer coefficient (K_L) and adsorption parameters required to quantify the possible gaseous mercury fluxes from these contaminated soils. Experimental results indicate that an equilibrium between the solid and gas phases was established. The proposed kinetic model reproduced perfectly the experimental data, with K_L found to be proportional to the inverse of temperature and independent of the radiation. The concentration of mercury in the gas phase was mainly dependent on the soluble mercury content (Hg_S). Equilibrium data were fitted by Langmuir and Freundlich models and the best fit was obtained using the multi-layer model attending to the convex shape of the curves, which is characteristic of non-porous or possibly macroporous materials having a low adsorption energy. The Freundlich constant (K_F) was also fitted as a polynomial function with temperature and this gave a straight line for the light radiation and a second grade equation for dark conditions. Once the parameters had been obtained, the Hg emission fluxes from contaminated soils were estimated and the values were between two and three orders of magnitude higher than those published in the literature for non-contaminated soils.

[a]Department of Chemical Engineering, University of Castilla-La Mancha, Avda. Camilo José Cela s/n, 13004 Ciudad Real, Spain
[b]Instituto de Geología Aplicada, Universidad de Castilla-La Mancha, EIMI Almadén, Pl. Manuel Meca, 1, 13400 Almadén, Ciudad Real, Spain
[c]Exploraciones Mineras S.A. (EM), Avenida Apoquindo 4775, Providencia, Santiago, Chile. E-mail: pablo.higueras@uclm.es
[d]Department of Environmental Sciences, Jozef Stefan Institute, Ljubljana, Slovenia

1 Introduction

Mercury is an element that has been extensively mined for industrial use. The main problem related to mercury today is its presence in the atmosphere. This presence facilitates dry and wet deposition and favours the formation of methylmercury, an extremely toxic compound that is bioaccumulated by fish.[1–4] This fact has been a major driving force for tighter control of mercury emissions into the atmosphere. As a consequence, industrialized countries have set control measures: for example, the European Community has implemented a 'European Directive on mercury', which states that since 2011 the surplus mercury from European industries must be stored under secure conditions without the possibility of being exported.[5]

Nevertheless, there are still numerous sources of atmospheric mercury, including the re-emission of previously deposited mercury originating from various anthropogenic and natural sources.[6] Regulations or methodologies to assess mercury emissions from soils, vegetation and water bodies have not been standardized or agreed. The commonly used techniques to determine mercury emission from soils involve the use of flow chambers or dynamic flux chambers and micro-meteorological methods.[7–12] However, differences in methodological experimental designs and operating parameters can significantly influence the results obtained with these techniques.[9] This problem is particularly significant for *in situ* measurements in areas enriched with mercury, where site heterogeneity significantly influences the magnitude of mercury fluxes.[10] In addition, there are a number of environmental parameters that can influence the emission rates, such as temperature, solar radiation and soil moisture content.[11–13] The form and mobility of mercury in soil are also important as they determine the pool of mercury available for volatilization.[14,15]

In this work we have developed a novel laboratory methodology for the quantification of mercury emissions from contaminated soils. All previous studies on this topic involved

the use of open systems, but in our case a closed circuit setup was designed in order to measure the amount of mercury desorbed and emitted from the soil during the time required to reach asymptotic equilibrium. Soil samples were subjected to two excitation factors: temperature and light radiation. The introduction of an external air flow was not required and flow variables that could influence the quantification of the emission were excluded. The experimental results enabled the equilibrium between mercury in the solid and gas phases to be calculated using the Langmuir and Freundlich models.[16] Once the equilibrium had been obtained, mercury fluxes from the soil to the gas phase were characterized by applying the mass transfer rate between the solid–gas interface on the basis of results obtained in other fields by different authors.[17–21] Samples were collected from the Almadén mercury mining district, located in South Central Spain, where the exploitation and extraction of mercury are traditional.[22–24] Soils adjacent to this area are heavily contaminated by mercury, as reported by other authors.[25–32]

The main objectives of this work were (i) to develop a mathematical model that describes the relationship between mercury concentrations in soil and air as a function of temperature and light radiation; and (ii) to develop a methodology to infer emissions of mercury from soils based on the knowledge of available mercury and excitation conditions (heat and radiation). The method should be applicable to soils with similar characteristics to those present in the study area.

2 Mathematical model

Different models have been applied in the literature to reproduce the equilibrium between phases, particularly when a solid material is involved. Langmuir and Freundlich equations have two fitting parameters and they are used for various gas–solid and liquid–solid systems.[16,33–35]

Once the sample in a closed circuit is under a stable thermodynamic condition, a proportion of the mercury contained in the soil passes directly to the gas phase, a change that increases the mercury concentration in the environment (confined air). The chemical equilibrium is described by eqn (1):

$$Hg_S \leftrightarrow Hg^* \tag{1}$$

where Hg_S is the available mercury concentration in the soil and Hg^* is the equilibrium concentration of mercury in the gas phase, which is in equilibrium with the solid phase.

The rate of mercury release from the contaminated soils to the gas phase can be written as follows:[35]

$$\frac{d(Hg)}{dt} = K_L a(Hg^* - Hg) \tag{2}$$

where Hg is the bulk average solute concentration in the gas ($ng\ m^{-3}$), K_L is the overall mass-transfer rate coefficient based on the gas-phase resistance ($m\ s^{-1}$) and a ($m^2\ m^{-3}$) is the soil area exposed to air per unit volume of the gas phase (V).

Eqn (2) is integrated with the boundary condition, $Hg = Hg^0$ at $t = 0$, where Hg^0 is the initial mercury concentration in the gas phase. The following expression is obtained upon integration:

$$Hg = Hg^* - (Hg^* - Hg^0)e^{-K_L at} \tag{3}$$

the volumetric gas–solid mass transfer coefficient $K_L a$ and equilibrium concentration of mercury in the gas phase Hg^* can be estimated by minimization of the squared difference between the mercury concentrations measured experimentally and those predicted by eqn (3).

The values of a and K_L are calculated by measuring the volume of the gas phase (reactor volume, V) and from the known value of the soil area exposed to air (S). K_L values depend on the flow regime, temperature, properties of both phases and the geometrical configuration.

Mass balance of mercury with mass transfer through the solid–gas interface for a contaminated area is represented as follows:

$$\frac{V}{S}\frac{d}{dt}Hg = \frac{1}{S}\frac{d}{dt}\ m_{Hg} = K_L(Hg^* - Hg^0) \tag{4}$$

where m_{Hg} is the total mass of mercury emitted from the soil in a contaminated area.

The amount of mercury emitted from the soil is negligible with respect to the total soil mercury concentration and the volume of air in the atmosphere is extremely large. As a result, Hg^* and Hg^0 are assumed to be independent of time. Hence, the total mass of mercury emitted into the atmosphere by a specific area as a function of time can be obtained by eqn (5):

$$m_{Hg} = K_L S(Hg^* - Hg^0)t \tag{5}$$

It can be seen from the above equations that in order to reproduce the mass of mercury emitted from contaminated soil to the atmosphere it is necessary to know the relationship between the equilibrium concentration of mercury in air (Hg^*) and the soil mercury concentration (q^*). As mentioned above, in this work two different adsorption equations have been tested in order to model the experimental data. The Langmuir eqn (6) is applicable for monolayer models, assuming that all active sites of the solid have the same affinity for the solute under investigation.[16,32]

$$q^* = \frac{Hg^* \times K_{Lang}(T)^* Q}{1 + K_{Lang}(T)Hg^*} \tag{6}$$

where Q is the maximum amount of mercury in the soil ($ng\ g^{-1}$ of dry soil) and K_{Lang} is the Langmuir equilibrium constant, which is dependent on the temperature.

The Freundlich eqn (7) is purely empirical but is widely used to describe adsorption systems with unlimited sorption sites.[32,33]

$$q^* = K_F(Hg^*)^{1/n} \tag{7}$$

where K_F and $1/n$ are empirical constants.

Several conclusions concerning adsorption can be drawn depending on the n values. For the case $n = 1$, the amount of solute adsorbed per unit of the adsorbent is proportional to the

equilibrium concentration Hg*, where K_F is the distribution or partition coefficient. For $n > 1$, the adsorption is weakly dependent on Hg* and for $n < 1$ the adsorption is strongly dependent on Hg*.

3 Materials and methods

The soil samples were taken in the context of a previous study by Martínez-Coronado et al.[32] The location corresponds to the so-called 'Cerco Metalúrgico de Almadenejos' (CMA) and its surroundings. CMA consists of a decommissioned metallurgical precinct, located 13 km from the ESE of Almadén and immediately to the North of the village of Almadenejos (Fig. 1). Samples taken from the 'A' horizon (0–10 cm depth) correspond to two different subareas: the interior of the precinct (samples Alce-) and the outskirts of the precinct (samples Al-). Soils inside the precinct correspond to anthrosols with generally high Hg concentrations, whereas outer soils were of diverse typology and showed much lower Hg concentrations.[32]

3.1 Determination of total mercury

The analysis of soil samples for total mercury was carried out at room temperature on dry samples, which were disaggregated and split into separate aliquots. The samples were ground to less than 100 μm size with an agate mortar. About 5 to 10 mg of the treated sample was used for analysis. For each sample, three replicates were analyzed using a LUMEX RA-915+ instrument. This equipment is based on Zeeman atomic absorption spectrometry, with high frequency modulation of light polarization (ZAAS-HFM).[36] Application of the Zeeman background correction and a multipath analytical cell provided high selectivity and sensitivity of measurements. Addition of the RP-91C (pyrolysis) attachment allowed Hg measurements on the soil samples: mercury in the samples was converted from a bound state to the atomic state by thermal decomposition at 700 °C in a two-section atomizer. The sample was first vaporized and the

mercury compounds were partly decomposed. The sample was subsequently heated to 800 °C, the point at which mercury compounds became fully decomposed and organic compounds and carbon particles were catalytically transformed to carbon dioxide and water. Each analysis took 1–2 min and the detection limit for total Hg was 0.5 ng g^{-1}. The equipment was calibrated using SRM reference standards (NIST 2710 and 2711) in total mercury concentration (32 600 and 6250 ng g^{-1}, respectively), which were also used periodically to check signal instrumental fluctuations with time. Quality control at the IGeA laboratory was achieved by analyzing equipment blanks (<0.002 mg kg^{-1}), duplicate samples (Relative Standard Deviation: 0.96%) and the certified reference material NIST SRM 2710 (32.6 mg kg^{-1} Hg), with acceptable precision (4.53%) and accuracy (98.65%) obtained for total mercury in solid samples under the analysis conditions.

3.2 Water-soluble mercury fraction

The water-soluble mercury fraction was determined in a previous study.[15] Determinations were based on the sequential extraction procedure proposed by Bloom et al.[37]

3.3 Experimental setup

The experimental setup is shown in Fig. 2 and consists of a jacketed and hermetically sealed Pyrex reactor with a volume of $V_R = 3.35 \times 10^{-3}$ m^3. The reactor was filled with air and contained the mercury polluted soil sample. The samples were encapsulated using a cylindrical polypropylene container with the aim of insulating the mercury flow from the perimetric and basal areas. All of the studied samples had a volume of $V_S = 0.129 \times 10^{-3}$ m^3 and an upper surface area of $S = 0.004902$ m^2, which is the part of the sample that interacts with the environment. Mercury released from the soil is accumulated in the reactor air, thus increasing in concentration until equilibrium is reached. The heating system is formed by a temperature-controlled thermostatic bath and the temperature was kept at
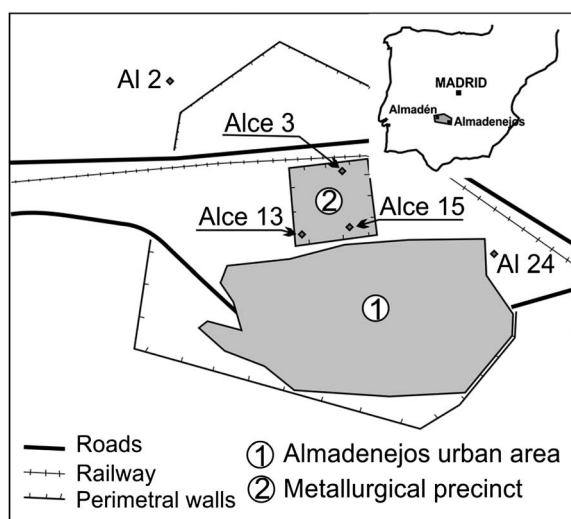

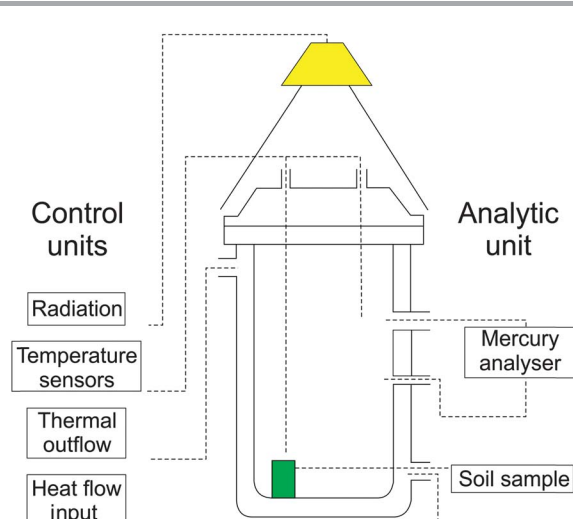**Fig. 1** Location and accessibility of the samples.

Fig. 2 Laboratory experimental setup for mercury emission quantification.

different values from 25 to 50 ± 1 °C. These studies were carried out in two ways: (i) study of the kinetics of mercury emissions considering only the influence of temperature by isolating the sample from light (dark conditions) and (ii) study of the kinetics of mercury emissions considering both temperature and radiation, by irradiating the system with artificial light provided by an ASD Inc. Illuminator Reflectance Lamp with a constant intensity of 32.6 klx (273 W m^{-2}). The lamp produced stable illumination over the 350–2500 nm range.

The increase in the gaseous mercury concentration inside the reactor was continuously measured with the LUMEX RA-915+ mercury analyzer, which had a working range from 2 to 20 000 ng m^{-3}. Analyses were carried out on the air passing through the analyzer closed system at a forced air flow of 12 L min^{-1}. The main difference from previous systems is that air is in a closed loop rather than being renewed or filtered.

4 Results and discussion

4.1 Quantification of total mercury (Hg$_T$) and soluble mercury (Hg$_S$)

The concentrations of total and water-soluble mercury reported by Martínez-Coronado et al. and Llanos et al. respectively are given in Table 1.[15,32] The sample notations are consistent with those reported by Martinez-Coronado et al.[32] These authors explained that high RDS values for both total and soluble Hg analyses were due to heterogeneity of the samples and not due to instrumental fluctuations.[15,32] It can be observed that higher concentrations of total mercury are directly related to the distance from the emission sources (metallurgical furnaces from the CMA precinct, see Fig. 1). This trend is also observed for the soluble mercury concentration for the samples denoted as 'Alce', which were collected from inside the metallurgical precinct. The maximum Hg$_S$ concentration, found in sample Alce3, could be due to lixiviation promoted by the rainwater coming from the land located in the upper part of the precinct.

4.2 Influence of temperature and radiation kinetics

As commented above, K_L is a function of the geometric configuration, the flow regime, the properties of both phases and the temperature. Bearing in mind that all of the experiments were carried out under the same conditions and also using the same installation, this parameter is only a function of temperature. Thus, in order to obtain reliable and meaningful values for K_L and Hg* for each temperature, all kinetic experiments under dark or light conditions were fitted by non-linear regression to the mathematical model previously described.

The kinetics data and modelling results achieved with the model described above are shown in Fig. 3 and 4; fitting parameters (K_L and Hg*) and the determination coefficient R^2 are shown in Table 2. It can be seen from the two figures that the proposed kinetic model reproduces perfectly the mercury emissions from soils into the atmosphere. Furthermore, determination coefficients with values close to unity confirm this as a good fit.

It can be seen from Fig. 3a and 4a that higher temperatures lead to higher mercury concentrations in the gas phase. These results are in agreement with observations made by Bahlmann et al. for both dark and light conditions, where the temperature increased the rate of flux of mercury to the gas phase from a contaminated soil.[11] The vapour pressure of highly volatile Hg^0 is increased by temperature and sorption by soil is decreased due to increasing thermal motion. An increase in the temperature also causes an increase in reaction rates and microbiological activity, resulting in a more intensive formation of volatile mercury species.[38] Previous studies carried out by Revis et al., in which natural soil samples containing 0.5 to
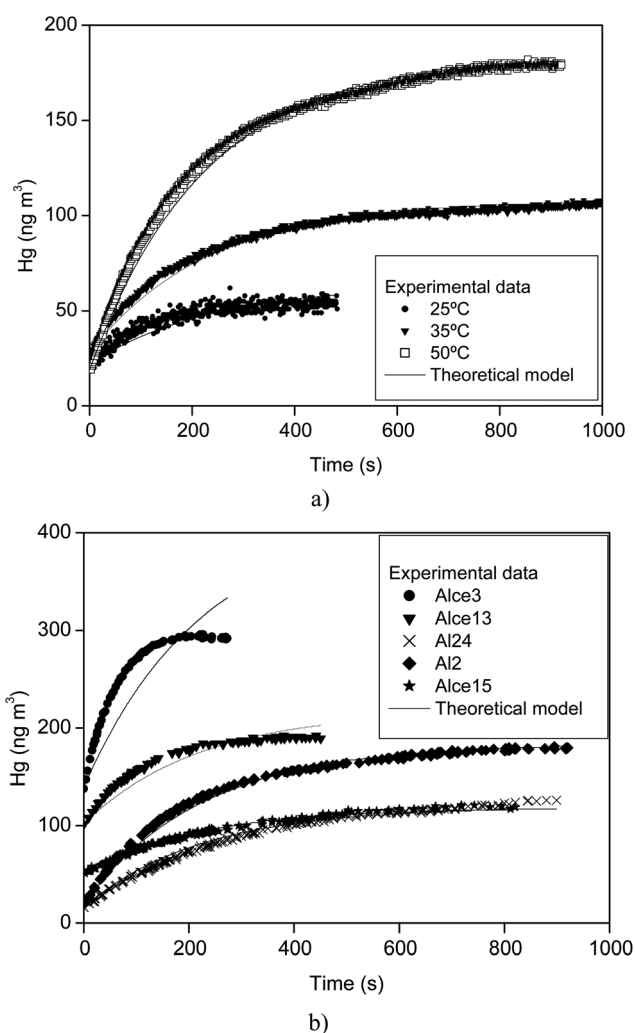

Fig. 3 Experimental and theoretical kinetics of mercury emissions under dark conditions; a): sample Al24; b): temperature 50 °C.

Table 1 Quantification of water-soluble (Hg$_S$ in ng g^{-1}) and total mercury (Hg$_T$ in mg kg^{-1}) for the studied samples; RSD: relative standard deviation (%)

Sample	Blank	Alce15	Al2	Al24	Alce13	Alce3
Replicates	2	3	3	3	3	3
Hg$_S$	0.050	20	35	50	60	4300
RSD Hg$_S$		36	76	8	46	68
Hg$_T$	…	700	75	170	1900	5500
RSD Hg$_T$		9	12	12	11	2

a)

b)

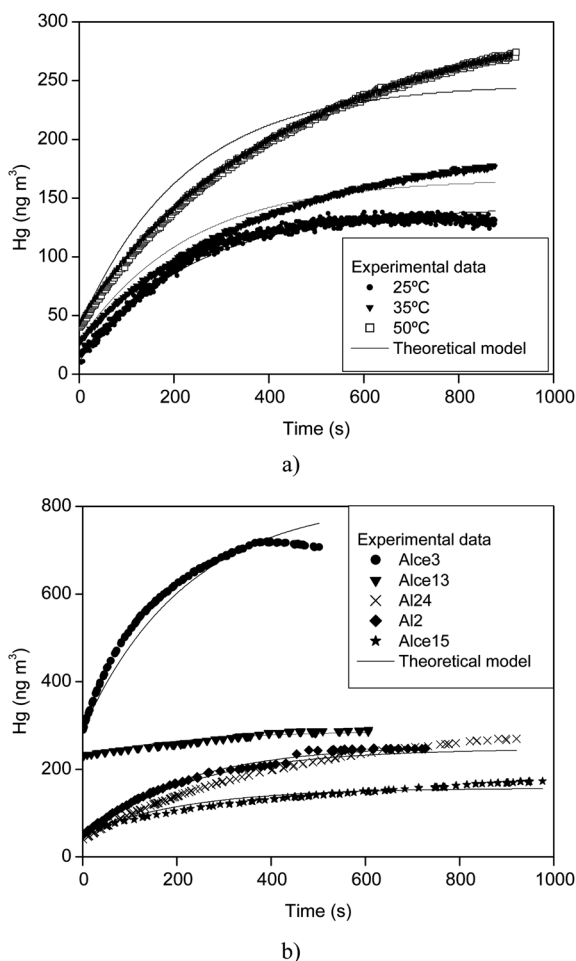**Fig. 4** Experimental and theoretical kinetics of mercury emissions under light conditions; a): sample Al24; b): temperature 50 °C.

3000 μg g^{-1} of total Hg [91% inorganic, 0.01% organic (as methyl Hg), and 6% Hg^0] were heated at 150 °C for 5 days, revealed that 98% of the volatilized mercury species was the initial elemental mercury (Hg^0); they also noted that the organic species was volatile.[39] Bloom *et al.* reported a high volatilization of different soluble species of mercury such as HgCl$_2$, Hg$_2$Cl$_2$ and Hg bonded to organic matter under the same environmental conditions.[37] This indicates that high temperatures stimulate the potential for mobility of mercury compounds in the sample, thus increasing its emission into the atmosphere. Thus, thermally controlled emission of mercury from soils is governed by the interfacial equilibrium of Hg^0 between the soil matrix and the gas phase.

These figures also show that the higher the experimental temperature the larger the slope of the kinetics curves, regardless of the radiation conditions. This finding is consistent with the mass transfer coefficients, which follow the order: $K_L^{50°C} > K_L^{35°C} > K_L^{25°C}$. The values of K_L given in Table 2 confirm this independence and its proportionality with temperature, with the straight-line $K_L(T) = 6.867 \times 10^{-6}T + 2.721 \times 10^{-3}$ obtained with an $R^2 = 0.998$. It can be seen from Fig. 3a how the gas phase concentration tends to be asymptotic for experimental times close to 600 seconds, a situation confirming that an equilibrium between the gas (Hg*) and solid phases has been established. In contrast, it can be seen from Fig. 4a that under light conditions the solid releases a higher amount of mercury and a longer time is required to achieve the equilibrium. This result is consistent with the independence of K_L values with respect to the radiation conditions, with the differences between the kinetics of mercury emission under dark and light conditions mainly related to the differences in the value of Hg*, which is higher for the light conditions.

Choi and Holsen reported that light radiation could increase the soil surface temperature and promote higher mercury emission from the soil surface.[38] The influence of this parameter is shown in Fig. 4, which shows that a higher level of mercury is emitted by the soil to the air compared to that under dark conditions. These results can be explained if different mercury species are formed during the photodecomposition of mercury compounds under light radiation, which substantially

Table 2 Mass transfer coefficients, mercury equilibrium concentration in the gas phase and R^2 for studied samples as a function of temperature. Analytical data taken from Llanos *et al.* (2011)

Temperature °C	Sample	Dark condition			Light condition		
		$K_L \times 10^3$ (m s^{-1})	Hg* (ng m^{-3})	R^2	$K_L \times 10^3$ (m s^{-1})	Hg* (ng m^{-3})	R^2
25 °C	Alce3	2.890	31.666	0.886	2.890	160.988	0.991
	Alce13		32.937	0.961		65.448	0.898
	Al24		63.820	0.792		141.910	0.983
	Al2		33.337	0.962		135.195	0.993
	Alce15		25.938	0.987		74.483	0.960
35 °C	Alce3	2.966	131.668	0.871	2.966	305.845	0.980
	Alce13		73.096	0.978		127.066	0.811
	Al24		107.972	0.884		166.221	0.957
	Al2		…	…		…	…
	Alce15		112.472	0.998		95.5906	0.905
50 °C	Alce3	3.062	413.991	0.589	3.062	817.068	0.949
	Alce13		218.071	0.873		288.006	0.930
	Al24		183.553	0.982		246.555	0.930
	Al2		118.484	0.991		255.128	0.987
	Alce15		119.267	0.987		157.255	0.924

increases the emission of this toxic element. This fact is a clear indication of the presence of mercury species in the soil that are susceptible to photodecomposition: Hg^+, Hg^{2+}, Hg^0.[40] Photocatalytic reduction of Hg^{2+} to volatile Hg^0 at the soil surface has been reported in numerous studies.[10,41–43] Gustin *et al.* demonstrated that light energy can be the dominant factor that controls mercury emission and that light-enhanced emission depends on the form of mercury in the substrate.[44]

4.3 Isotherm models

It can be seen from the results in Table 2 that the higher the Hg_S in the soil, the higher the mercury emitted to the atmosphere, with the maximum emission observed for sample Alce13. This relationship is not observed when total mercury is considered, since samples with high Hg_T presented lower emissions compared to samples with lower contents. The reason for this effect is the known interaction of the soluble mercury fraction with the environment, with the element evaporating initially as Hg^0 followed by other mercury species.[37,39] Thus, it is possible to establish a relationship between Hg_S and Hg^*, with Hg_S considered as the soil mercury concentration at equilibrium (q^*). Values of Hg^* and q^* were fitted to the Langmuir and Freundlich models as functions of temperature and light radiation.

The fitting parameters of the Langmuir and Freundlich equations (Q, K_{Lang}) and (K_F, n), respectively, are shown in Table 3. It is also important to point out that only natural soils (Alce15, Al2 and Al24) follow perfectly the proposed model whereas soils with heavier contamination (Alce3 and Alce13) show a significant deviation, with the equilibrium conditions for Alce3 included at the highest temperature and sample Alce13 was discarded for this purpose. The reason for the highest deviation for Alce3 with respect to the adsorption model could be related to the different form of mercury promoted by the uptake of lixiviates from the topographically higher area, as noted above.

As can be observed, the coefficient of determination R^2 is closer to unity on using the Freundlich model, particularly for light conditions, indicating that the soils present a multilayer behaviour. A worse fitting was achieved for dark conditions but this deviation is not unexpected when heterogeneous soils and not synthetic materials are studied. The maximum mercury uptake by the soil $Q \cong 3764$ ng g^{-1} obtained by applying the Langmuir model is only 11% lower than the soluble mercury

concentration from sample Alce3 ($Hg_S = 4300$ ng g^{-1}), indicating that this adsorption model could be used to reproduce the mercury equilibrium established between gas and solid phases.

The equilibrium data and the theoretical curves obtained using the Freundlich model are presented in Fig. 5. These curves agree well with the adsorption properties, because this phenomenon is not enhanced with temperature. Besides, it was also confirmed that, in the case of radiation, light promotes the photodecomposition of mercury, thus increasing the total mercury released from the soil and subsequently accumulated by air. The convex shape of the curves allows the adsorption isotherm to be classified as Type III, which is characteristic of non-porous or possibly macroporous materials that have a low energy of adsorption. This behaviour is also confirmed by the Freundlich parameter ($n = 0.651$), which is less than 1, indicating that the adsorption is strongly dependent on Hg^*.

It can be seen from the results in Table 3 that K_F could be related to the temperature, as a straight line is obtained for the light conditions $K_F(T) = 7.073 \times 10^{-1}T^{-1} - 3.830^{-3}$ with $R^2 = 0.968$ and the following quadratic function is obtained for dark conditions $K_F(T) = 2.495 \times 10^2 T^{-2} - 11.0 T^{-1} + 1.365 \times 10^{-1}$. Thus, once the mass transfer coefficients and the equilibrium parameters have been obtained, the mercury emissions from contaminated soils as a function of temperature and the soluble mercury content of the soil can be estimated.

4.4 Emission quantification

The Hg emission fluxes (HgEF) as functions of temperature and radiation are quantified using eqn (8) (derived from eqn (5)), which reflects the amount of mercury volatilized for a given surface per unit time. In this equation q^* was replaced by Hg_S because, as mentioned above, they are effectively the same.

$$\text{HgEF} = \frac{m\text{Hg}}{St} = K_L(T)\left(\left(\frac{\text{Hg}_S}{K_F(T)}\right)^n - \text{Hg}^0\right) \quad (8)$$

Assuming that Hg^0 is close to zero, then:

$$\text{HgEF} = K_L(T)\left(\frac{\text{Hg}_S}{K_F(T)}\right)^n \quad (9)$$

Pyrex glass only allows 87% of the total radiation to pass through and the total radiation due to the lamp was therefore

Table 3 Freundlich and Langmuir adsorption model parameters

Radiation	T °C	Freundlich $K_F \times 10^2$ (ng g^{-1}) (m^3 ng^{-1})$^{1/n}$	n	R^2	Langmuir $K_{Lang} \times 10^5$ (m^3 ng)	Q (ng g^{-1})	R^2
Dark	25	9.559	0.651	0.427	22.381	3763.632	0.849
	35	2.580		0.480	7.916	3763.675	0.410
	50	1.624		0.842	6.937	3763.403	0.817
Light	25	2.383		0.803	8.104	3763.672	0.823
	35	1.786		0.930	6.977	3764.633	0.814
	50	0.947		0.807	4.80	3764.633	0.691
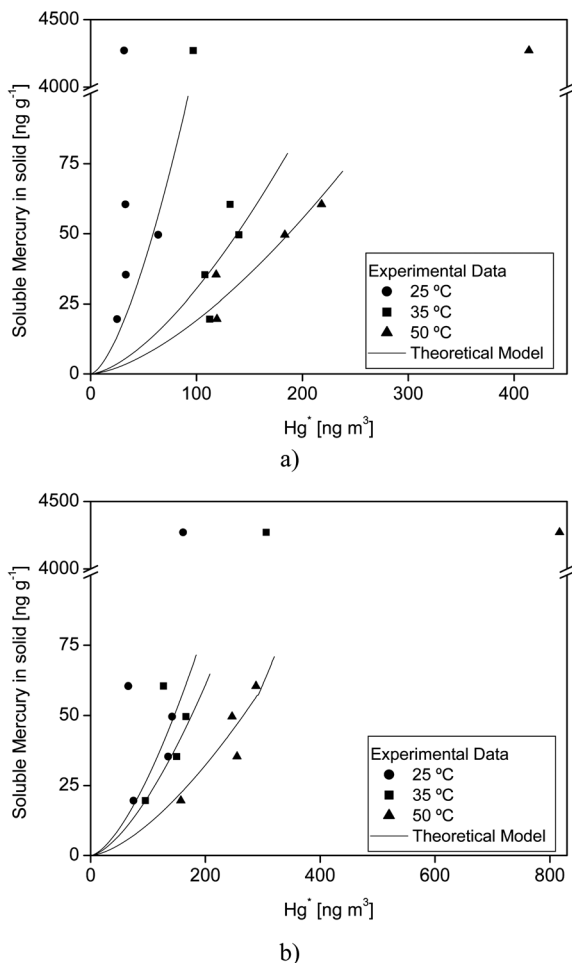
Fig. 5 Mercury adsorption isotherms; a): Dark condition; b): Light condition.

Fig. 6 Hg emission fluxes emitted to the atmosphere by contaminated soils from Almadén mercury mining district; a): Dark condition; b): Light condition at 273 W m^{-2}.

underestimated.[38] The real light contribution can be obtained by subtracting HgEF under dark conditions from the HgEF under light conditions. Furthermore, the mercury flux independent of the container material could be quantified by taking into account the amount of energy filtered out by the container with respect to the energy emitted by the source (E_{Source}/$E_{Filtered}$).

$$\text{HgEF} = K_L(T)\left[\left(1 - \frac{E_{Source}}{E_{Filtered}}\right)\left(\frac{\text{Hg}_S}{K_F(T)}\right)^n\Bigg|_{Dark} + \frac{E_{Source}}{E_{Filtered}}\left(\frac{\text{Hg}_S}{K_F(T)}\right)^n\Bigg|_{Light}\right] \quad (10)$$

when the energy source is zero, the mercury flux is only due to the dark conditions. For this work the source and the filtered energies were 273 and 237.51 W m^{-2}, respectively.

The mass flow rates of mercury emitted per hour for both radiation conditions as functions of the soil mercury content and temperature are shown in Fig. 6. It can be seen that the temperature makes a greater contribution than Hg$_S$ to HgEF. It can also be confirmed that desorption is strongly temperature dependent and increases with temperature. Comparison of the two figures shows that the participation of light increases the
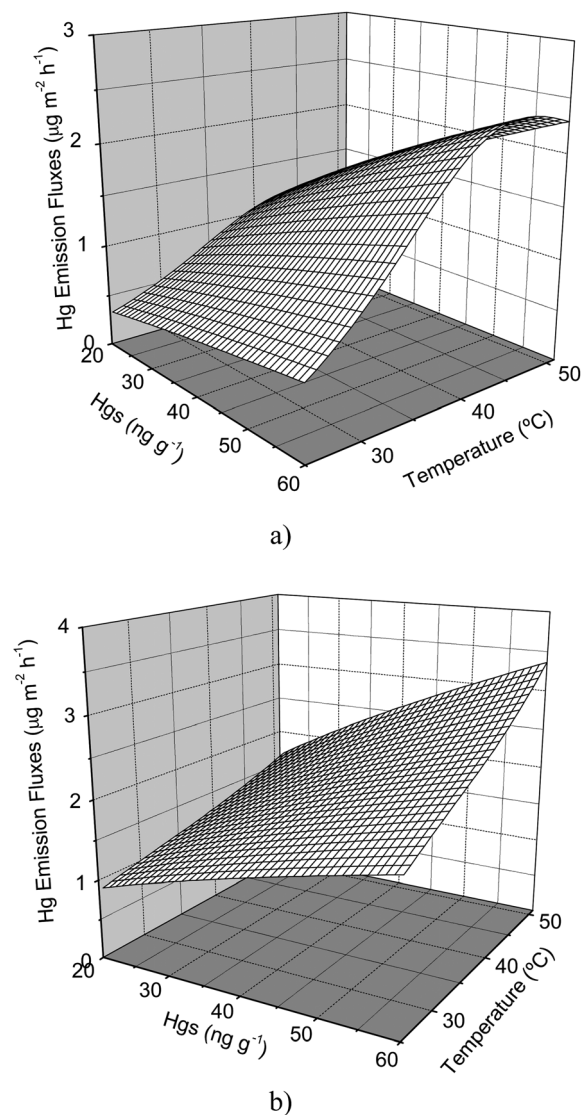
mass flow rates of mercury from contaminated soils in the range from 50% to an order of magnitude with respect to dark conditions.

Gaseous mercury fluxes ranging from 2.5 to 27.2 ng Hg^0 m^{-2} h^{-1} have been reported by Choi and Holsen for non-contaminated soils in the Adirondack Mountains of New York.[38] These mercury fluxes are three orders of magnitude lower than the ones reported in this article for an Hg mining district.

5 Conclusions

Quantification of mercury emissions in a closed circuit allowed the determination of the real emission of mercury from soils without the use of an additional air flow rate, which could interfere in the calculation of emissions. Experimental results indicate that the equilibrium between the solid and gas phases was established because the concentration of the accumulated

mercury in the gas phase tended to be constant. The kinetic model obtained using the mass transfer coefficient and the equilibrium concentration of mercury as fitting parameters reproduced the kinetic curves accurately. It was found that the mass transfer coefficient (K_L) was only dependent on the temperature. The equilibrium data showed a better correlation between the soluble mercury content (Hg_S) and the mercury concentration in the gas phase at equilibrium than with total mercury content (Hg_T). The convex shape of the adsorption isotherms allowed the adsorption isotherm to be classified as Type III, which is characteristic of non-porous or possibly macroporous materials with a low energy of adsorption.

These results confirmed that temperature and light radiation favour mercury desorption due to the increase in the mercury vapour pressure and also the possible photocatalytic reduction of soluble Hg^{2+} to volatile Hg^0 at the soil surface. Thus, the use of the theoretical kinetic model based on the physicochemical phenomena allows one to obtain the Hg emission fluxes from contaminated soils. For this purpose, the determination of two unknown parameters, *i.e.* (i) the mass transfer coefficient and (ii) the mercury concentration at equilibrium in the gas phase, was required. These parameters were related to the temperature and the soluble mercury content, respectively.

Finally, it was observed that the Hg emission fluxes obtained in this work were between two and three orders of magnitude higher than those published in the literature for non-contaminated soils. This trend indicates that it is very important to address the contamination of soil by mercury in the Almadén mining district.

Acknowledgements

References

1 W. H. Schroeder and J. Munthe, Atmospheric mercury—an overview, *Atmos. Environ.*, 1998, **32**, 809–822.

2 H. M. Chan, A. M. Scheuhammer, A. Ferran, C. Loupelle, J. Holloway and S. Weech, Impacts of mercury on freshwater fish-eating wildlife and humans, *Hum. Ecol. Risk Assess.*, 2003, **9**, 867–883.

3 L. T. Kurland, S. N. Faro and H. Siedler, The outbreak of a neurologic disorder in Minamata, Japan, and its relationship to the ingestion of seafood contaminated by mercury compounds, *World Neurol.*, 1960, **1**, 370–395.

4 Y. Takizawa, Understanding Minamata disease and strategies to prevent further environmental contamination by methylmercury, *Water Sci. Technol.*, 2000, **42**, 139–146.

5 K. J. Lee and T. G. Lee, A review of international trends in mercury management and available options for permanent or long-term mercury storage, *J. Hazard. Mater.*, 2012, **241–242**, 1–13.

6 N. Pirrone, S. Cinnirella, X. Feng, R. B. Finkelman, H. R. Friedli, J. Leaner, R. Mason, A. B. Mukherjee, G. Stracher, D. G. Streets and K. Telmer, Global mercury emissions to the atmosphere from anthropogenic and natural sources, *Atmos. Chem. Phys.*, 2010, **10**, 5951–5964.

7 Z. F. Xiao, J. Munthe, W. H. Schroeder and O. Lindqvist, Vertical fluxes of volatile mercury over forest soil and lake surfaces in Sweden, *Tellus*, 1991, **43B**, 267–279.

8 K. H. Kim and S. E. Lindberg, Micrometeorological measurements of mercury vapor fluxes over background forest soils in eastern Tennessee, *Atmos. Environ.*, 1995, **29**, 267–282.

9 C. S. Eckley, M. Gustin, C.-J. Lin, X. Li and M. B. Miller, The influence of dynamic chamber design and operating parameters on calculated surface-to-air mercury fluxes, *Atmos. Environ.*, 2010, **44**, 194–203.

10 M. S. Gustin, S. E. Lindberg, F. Marsik, A. Casimir, R. Ebinghaus, G. Edwards, C. Hubble-Fitzgerald, J. G. Kemp, H. H. Kock, T. Leonard, J. London, M. Majewski, C. Montecinos, J. Owens, M. Pilote, L. Poissant, P. M. Rasmussen, F. Schaedlich, D. Schneeberger, W. Schroeder, J. Sommar, R. Turner, V. Vette, D. Wallschlager, Z. W. Xiao and H. Zhang, Nevada STORMS project: measurement of mercury emissions from naturally enriched surfaces, *J. Geophys. Res.*, 1999, **104**, 21831–21844.

11 E. Bahlmann, R. Ebinghaus and W. Ruck, Development and application of a laboratory flux measurement system (LFMS) for the investigation of the kinetics of mercury emissions from soils, *J. Environ. Manage.*, 2006, **81**, 114–125.

12 J. Rinklebe, A. During, M. Overesch, G. Du Laing, R. Wennrich, H.-J. Stärk and S. Mothes, Dynamics of mercury fluxes and their controlling factors in large Hg-polluted floodplain areas, *Environ. Pollut.*, 2010, **158**, 308–318.

13 H. Zhang, S. E. Lindberg, F. J. Marsik and G. J. Keeler, Mercury air/surface exchange kinetics of background soils of the Tahquamenon River watershed in the Michigan upper peninsula, *Water, Air, Soil Pollut.*, 2001, **126**, 151–169.

14 A. D. Jew, C. S. Kim, J. J. Rytuba, M. S. Gustin and G. E. Brown, New technique for quantification of elemental Hg in mine wastes and its implications for mercury evasion into the atmosphere, *Environ. Sci. Technol.*, 2011, **45**, 412–417.

15 W. Llanos, D. Kocman, P. Higueras and M. Horvat, Mercury emissions and dispersion models from soils contaminated by cinnabar mining and metallurgy, *J. Environ. Monit.*, 2011, **13**, 3460–3468.

16 Langmuir, Chemical reactions at low pressures, *J. Am. Chem. Soc.*, 1915, **37**, 1139–1167.

17 M. Carmona, M. Khemis, J.-P. Leclerc and F. Lapicque, A simple model to predict the removal of oil suspensions from water using the electrocoagulation technique, *Chem. Eng. Sci.*, 2006, **61**, 1237–1246.

18 J.-B. W. P. Loos, P. J. T. Verheijen and J. A. Moulijn, Improved estimation of zeolite diffusion coefficients from zero-length column experiments, *Chem. Eng. Sci.*, 2000, **55**, 51–65.

19 M. Eic and D. M. Ruthven, A new experimental technique for measurement of intracrystalline diffusivity, *Zeolites*, 1988, **8**, 40–45.

20 J. Silva and A. Rodrigues, Sorption and diffusion of *n*-pentane in pellets of 5A zeolite, *Ind. Eng. Chem. Res.*, 1997, **36**, 493–500.

21 J. F. Rodriguez, J. L. Valverde and A. Rodrigues, Measurements of effective self-diffusion coefficients in a gel-type cation exchanger by the zero-length-column method, *Ind. Eng. Chem. Res.*, 1998, **37**, 2020–2028.

22 A. Hernández, M. Jébrak, P. Higueras, R. Oyarzun, D. Morata and J. Munhá, The Almadén mercury mining district, Spain, *Miner. Deposita*, 1999, **34**, 539–548.

23 P. Higueras, R. Oyarzun, R. Lunar, J. Sierra and J. Parras, The Las Cuevas deposit, Almadén district (Spain): an unusual case of deep-seated advanced argillic alteration related to mercury mineralization, *Miner. Deposita*, 1999, **34**, 211–214.

24 M. Jébrak, P. Higueras, E. Marcoux and S. Lorenzo, Geology and geochemistry of high-grade, volcanic rock-hosted, mercury mineralisation in the Nuevo Entredicho deposit, Almadén district, Spain, *Miner. Deposita*, 2002, **37**, 421–432.

25 S. E. Lindberg, D. R. Jackson, J. W. Huckabee, S. A. Janzen, M. J. Levin and J. R. Luna, Atmospheric emission and plant uptake of mercury form agricultural soils near the Almadén mercury mine, *J. Environ. Qual.*, 1979, **8**, 572–578.

26 P. Higueras, R. Oyarzun, H. Biester, J. Lillo and S. Lorenzo, A first insight into mercury distribution and speciation in soils from the Almadén mining district, *J. Geochem. Explor.*, 2003, **80**, 95–104.

27 P. Higueras, R. Oyarzun, J. Lillo, J. C. Sánchez-Hernández, J. A. Molina, J. M. Esbrí and S. Lorenzo, The Almadén district (Spain): anatomy of one of the world's largest Hg-contaminated sites, *Sci. Total Environ.*, 2006, **356**, 112–124.

28 J. E. Gray, M. E. Hines, P. Higueras, I. Adatto and B. K. Lasorsa, Mercury speciation and microbial transformations in mine wastes, stream sediments, and surface waters at the Almadén mining district, Spain, *Environ. Sci. Technol.*, 2004, **38**, 4285–4292.

29 J. A. Molina, R. Oyarzun, J. M. Esbrí and P. Higueras, Mercury accumulation in soils and plants in the Almadén mining district, Spain: one of the most contaminated sites on Earth, *Environ. Geochem. Health*, 2006, **28**, 487–498.

30 R. Millán, R. Gamarra, T. Schmid, M. J. Sierra, A. J. Quejido, D. M. Sánchez, A. I. Cardona, M. Fernández and R. Vera, Mercury content in vegetation and soils of the Almadén mining area (Spain), *Sci. Total Environ.*, 2006, **368**, 79–87.

31 W. Llanos, P. Higueras, R. Oyarzun, J. M. Esbrí, M. A. López-Berdonces, E. M. García-Noguero and A. Martínez-Coronado, The MERSADE (European Union) project: testing procedures and environmental impact for the safe storage of liquid mercury in the Almadén district, Spain, *Sci. Total Environ.*, 2010, **408**, 4901–4905.

32 A. Martínez-Coronado, R. Oyarzun, J. M. Esbrí, W. Llanos and P. Higueras, Sampling high to extremely high Hg concentrations at the Cerco de Almadenejos, Almadén mining district (Spain): the old metallurgical precinct(1794 to 1861 AD) and surrounding areas, *J. Geochem. Explor.*, 2011, **109**, 70–77.

33 J. M. Chern and Y. W. Chien, Adsorption of nitrophenol onto activated carbon: isotherms and breakthrough curves, *Water Res.*, 2002, **36**, 247–255.

34 H. Freundlich and W. Heller, On adsorption in solution, *J. Am. Chem. Soc.*, 1939, **61**, 2228.

35 R. Bandaru and P. Ghosh, Mass transfer of chlorobenzene in concentrated sulfuric acid, *Int. J. Heat Mass Transfer*, 2011, **54**, 2245–2252.

36 S. Sholupov, S. Pogarev, V. Ryzhov, N. Mashyanov and A. Stroganov, Zeeman atomic absorption spectrometer RA-915+ for direct determination of mercury in air and complex matrix samples, *Fuel Process. Technol.*, 2004, **85**, 473–485.

37 N. S. Bloom, E. Preus, J. Katon and M. Hiltner, Selective extractions to assess the biogeochemically relevant fractionation of inorganic mercury in sediments and soils, *Anal. Chim. Acta*, 2003, **479**, 233–248.

38 H. D. Choi and T. M. Holsen, Gaseous mercury fluxes from the forest floor of the Adirondacks, *Environ. Pollut.*, 2009, **157**, 592–600.

39 N. W. Revis, T. R. Osborne, G. Holdsworth and C. Hadden, Distribution of mercury species in soil from a mercury-contaminated site, *Water, Air, Soil Pollut.*, 1989, **45**, 105–113.

40 A. Davis, N. S. Bloom and S. Q. Hee, The environmental geochemistry and bioaccessibility of mercury in soils and sediments: a review, *Risk Anal.*, 1997, **17**, 557–569.

41 A. Carpi and S. E. Lindberg, Application of a Teflon® dynamic flux chamber for quantifying soil mercury flux: tests and results over background soil, *Atmos. Environ.*, 1998, **32**, 873–882.

42 A. Gillis and D. R. Miller, Some potential errors in the measurement of mercury gas exchange at the soil surface using a dynamic flux chamber, *Sci. Total Environ.*, 2000, **260**, 181–189.

43 A. Gillis and D. R. Miller, Some local environmental effects on mercury emission and absorption at a soil surface, *Sci. Total Environ.*, 2000, **260**, 191–200.

44 M. S. Gustin, H. Biester and C. Kim, Investigation of light enhanced emissions of mercury from naturally enriched substrate, *Atmos. Environ.*, 2002, **36**, 3241–3254.